

Preparation and biomedical application of a non-polymer coated superparamagnetic nanoparticle

Lin Du¹
 Jianzhao Chen¹
 Yanting Qi¹
 Dan Li¹
 Chonggang Yuan¹
 Marie C Lin³
 David T Yew⁴
 Hsiang-Fu Kung⁵
 Jimmy C Yu²
 Lihui Lai¹

¹Institute of Molecular and Chemical Biology, East China Normal University, Shanghai, China; ²Department of Chemistry, The Chinese University of Hong Kong, Hong Kong, China; ³Department of Chemistry, Open Laboratory of Chemical Biology of the Institute of Molecular Technology for Drug Discovery and Synthesis, The University of Hong Kong, Pokfulam, Hong Kong, China; ⁴Department of Anatomy, Faculty of Medicine, The Chinese University of Hong Kong, Hong Kong, China; ⁵Centre for Emerging Infectious Diseases, Faculty of Medicine, The Chinese University of Hong Kong, China

Abstract: We report the preparation of a non-polymer coated superparamagnetic nanoparticle that is stable and biocompatible both in vitro and in vivo. The non-polymer, betaine, is a natural methylating agent in mammalian liver with active surface property. Upon systemic administration, the nanoparticle has preferential biodistribution in mammalian liver and exhibits good reduction of relaxivity time and negative enhancement for the detection of hepatoma nodules in rats using MRI. Our data demonstrate that the non-polymer coated superparamagnetic nanoparticle should have potential applications in biomedicine.

Keywords: SPIO nanoparticle, betaine, hepatoma, MRI

Introduction

The applications of superparamagnetic iron oxide nanoparticles (SPIO) in biomedicine have been actively pursued in recent years (Wilkinson 2003; Gupta and Gupta 2005; Hu and Yu 2006). However, relatively little work has been carried out on the non-polymer coated superparamagnetic nanoparticles with entire size smaller than 10 nm. It has been demonstrated that the size of iron oxide particle and the coating have a notable influence on its magnetic property, cellular uptake and cell viability. Generally speaking, the nanoparticles employed for in vivo applications should be sufficiently small, stable at physiological condition without aggregation and present superparamagnetic behavior at room temperature. All SPIO nanoparticles presently undergoing preclinical or clinical testing are coated with polymeric material (eg, dextran, carboxydextran, polyethylene glycol). Dextran limits the tolerance of the compound, which can therefore only be administered as a slow infusion (Panyam and Labhasetwar 2003). In fact, all polymers used, even the well-tolerated polyethylene glycol, have limitations in tissue distribution, penetration, metabolic clearance and produce adverse reactions (Zhang et al 2002).

Recently, a non-polymer (citrate) coated superparamagnetic nanoparticle has been investigated in MR angiography (Schnorr et al 2002; Taupitz et al 2000; Wagner et al 2002). Here we report a non-polymer coated SPIO nanoparticle, which has an overall size around 9 nm and is stable and biocompatible both in vitro and in vivo. Following systemic administration, the nanoparticle has preferential biodistribution in mammalian liver and exhibits good reduction of relaxivity time and negative enhancement for the detection of hepatoma nodules in a rat model using magnetic resonance imaging (MRI).

The surface chemistry of nanoparticles is important for their potential applications in biomedicine. In this report, we use betaine as a stabilizing agent for the preparation of SPIO nanoparticles. We choose betaine for this purpose based on the following considerations: (1) betaine is a molecule comprising amphiphilic character, which is stable over a wide pH range in biological conditions; (2) betaine is a natural methylating agent in mammalian liver, which has been found to protect the livers of experimental animals

Correspondence: Lihui Lai
 Institute of Molecular and Chemical Biology, East China Normal University,
 N. 3663 Zhongshan Rd., Shanghai 200062,
 China
 Tel/Fax +86 6223 7226
 Email lhilai@bio.ecnu.edu.cn

against the hepatotoxic ethanol and carbon tetrachloride; and (3) betaine is an effective hydrotrope with small size, which possesses well-tolerated in tissue penetration and metabolic clearance in vivo (Barak et al 1996). The aim of this study is to generate betaine coated SPIO nanoparticle and investigate its potential applications in vivo. Our preliminary data demonstrate that the non-polymer coated nanoparticle is useful as an MRI contrast agent.

Methods and results

Preparation and characterization of SPIO nanoparticles

For the preparation of magnetite nanoparticles, 1 M $\text{FeCl}_3 \cdot 6\text{H}_2\text{O}$ (>99%) was mixed with 2 M $\text{FeCl}_2 \cdot 4\text{H}_2\text{O}$ (>99%) at the ratio 2:1 and then 28.6% (w/w) Betaine hydrochloride (Fluka Biochemika) was dissolved in the solution by stirring. The pH of reaction solution was adjusted

with the 3M NaOH until reaching a pH value of 11. After stirring vigorously for 15 min, the solution pH was adjusted to 4 by adding 2M HCl dropwise. The betaine coated Fe_3O_4 particles were collected by magnetic separation by applying a permanent magnet for 30 min and washed with deionized water three times. To remove excess ions and betaine further, the product was dialyzed against with deionized water overnight. Following this, the solution was centrifuged at 3500 g at RT for 10 min. Finally the product was passed through a 0.22 μm filter and used for investigations. Electron micrographs of the magnetite dispersions were carried out using a drop of the sample onto a copper mesh coated with an amorphous carbon film. This mesh was then dried in a vacuum desiccator. TEM images were performed using a type JEOL-JEM-100-CXII with working condition 100 kV. Figure 1a shows a TEM image of the iron oxide suspensions with a well-dispersed feature.

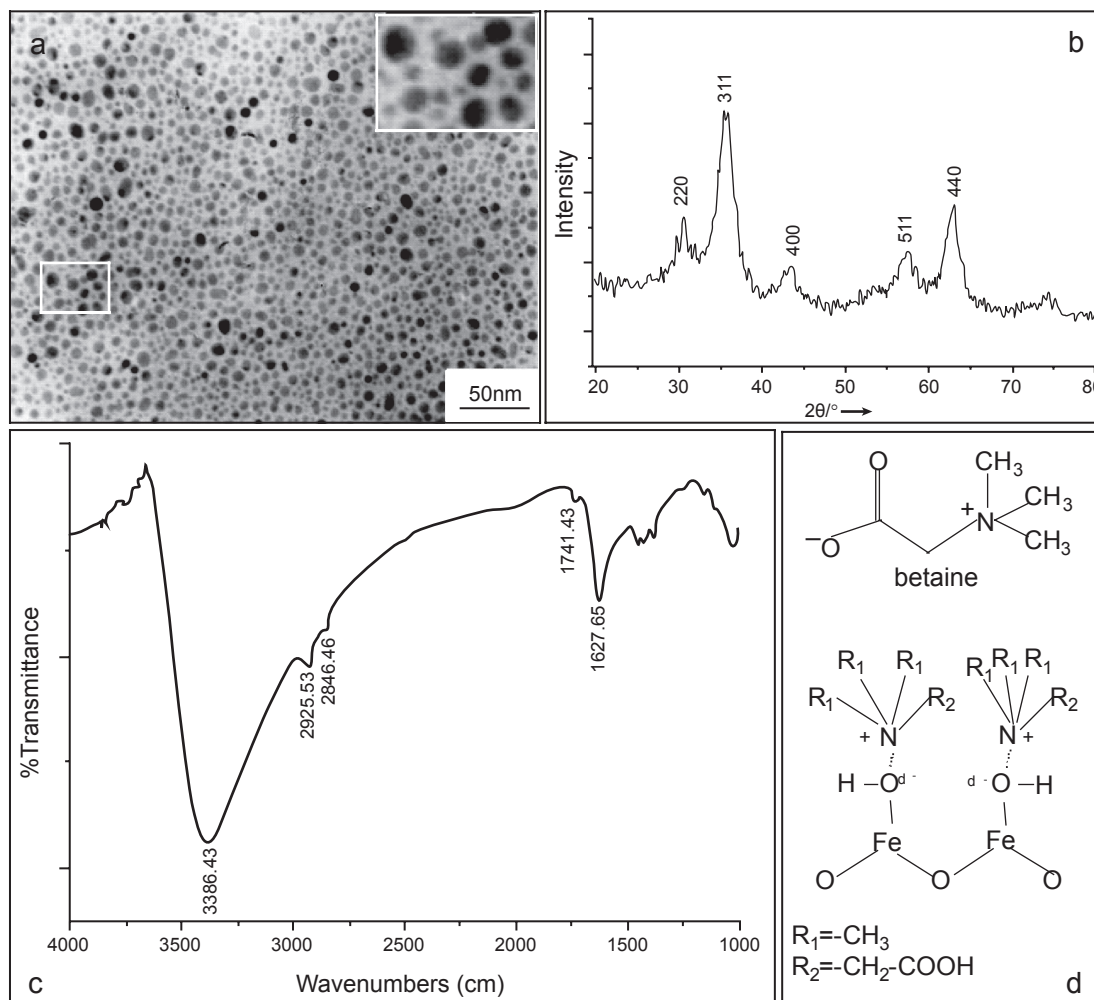


Figure 1 Characterization of the SPIO nanoparticle. (a) TEM image of the SPIO nanoparticles from the as-synthesized colloidal suspensions following centrifugation at 10,000 rpm, Bar 50 nm, magnification 20,000 \times , (b) X-ray powder diffraction patterns of the SPIO nanoparticles, (c) FT-IR spectrum of the SPIO nanoparticles, and (d) chemical structure of betaine (above) and the proposed electrostatic interaction of the betaine with Fe_3O_4 (below).

To characterize the products further, partial products were dried in vacuum oven at 25 °C for 12 h and used for X-ray diffraction (XRD) analysis (Taupitz et al 2002). XRD data were collected on a Rigaku D/max 2550 V X-ray diffractometer employing Cu-K α radiation ($\lambda = 1.54056$ Å at 40 kV and 100 mA). Figure 1b displays the XRD patterns for the as-precipitated powders corresponding to Figure 1a. As magnetite (Fe₃O₄) may be converted to maghemite (gamma Fe₂O₃) in the presence of oxygen, it is possible that the core of the resulting nanoparticles can consist of maghemite as it has been demonstrated recently (Thünemann et al 2006).

The surface properties were characterized using FT-IR. The iron oxide precipitates were dried and ground with KBr for IR measurements by a Nexus 670 FT-IR spectrophotometer with a resolution of 2 cm⁻¹. FT-IR analysis was performed to characterize the surface nature of the resulting magnetite nanoparticles, as depicted in Figure 1c. A vibrational feature at 1628 cm⁻¹ is found and assigned to the C–N stretching motion, which could be derived from betaine that was coated on Fe₃O₄. The broad peak appeared in the region 3200–3600 cm⁻¹ region corresponds to the O–H stretching vibration as the iron oxide surfaces are readily covered with hydroxyl groups in an aqueous environment (Cheng et al 2005). The proposed electrostatic interaction of the betaine with Fe₃O₄ was shown in a scheme in Figure 1d.

To investigate the magnetic properties of the SPIO nanoparticle, magnetization measurements have been made at 23 °C with respect to the particle size using a vibrating sample magnetometer (VSM, JDM-13) at $-18000 \text{ Oe} \leq H \leq 18000 \text{ Oe}$. The superparamagnetic behavior of the SPIO nanoparticle was evidenced by zero coercivity and remanence on the magnetization loop and a saturation magnetization of 56.8 emu/g was determined (Figure 2a). The Fe₃O₄ concentrations were measured by treating the iron oxides with nitric acid and were calculated on the basis of the average diameter of the iron oxide particles. Moreover, a 0.3T NMR spectrometer with an extremity 5 cm coil was used for the r1; r2 measurement of SPIO nanoparticles in the water. The T1 and T2 measurements were carried out using the inversion recovery and Carr-Purcell-Meiboom-Gill (CPMG) sequences, respectively. Samples were dissolved into deionized water and were analyzed for subsequent determination of the r1 and r2 properties. The commercial Gd-DTPA was also analyzed for a comparative study. At a concentration of 0.1 mM of the magnetite particles, the longitudinal relaxation time (T1) was reduced from 2117 ms for pure water to 408 ms (Figure 2b), while the T2 relaxation time was reduced from 2039 to 108

ms (Figure 2c). A comparison of T1 and T2 values of ddH₂O, Gd-DTPA and SPIO that were measured using each pulse for refocusing in the multiecho sequence is given in Table 1. Our data demonstrated that the SPIO nanoparticle strongly reduced both T1 and T2 relaxation times with T2 significantly lower than T1. Therefore, this particle may have the potential for MR imaging as a contrast agent.

Cytotoxicity evaluation

Cell lines including SMMC-7721 and HL7702 were cultured in DME medium supplemented with 10% fetal bovine serum, 2 mm l-glutamine and 50 mg/ml gentamicin at 3×10^4 cells/well in 24-well plates at 37 °C under a humidified atmosphere of 95% air and 5% CO₂. After 24 h, the cells were applied with serial 5-fold dilutions of the SPIO nanoparticle and Gd-DTPA (Schering AG, Germany) in triplicate with final concentrations ranging from 0.2 to 5 mM for 4 h. Following replenishment with fresh medium, the cells were incubated for addition 48 h. Histochemistry analysis was carried out with Prussian blue staining for the presence of iron. Figure 4a

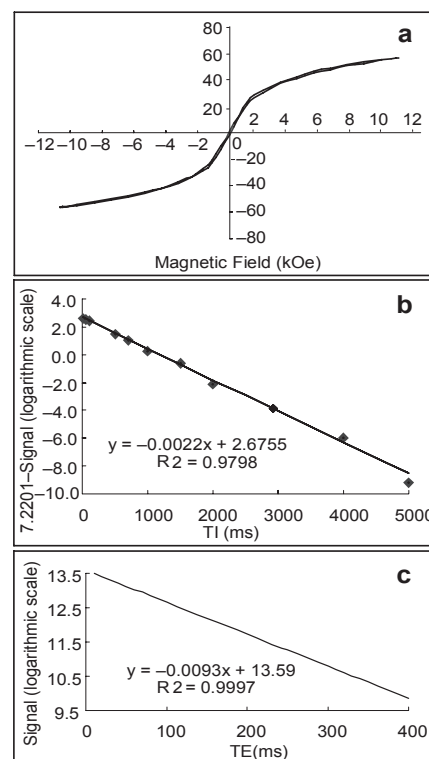


Figure 2 Magnetic properties of the SPIO nanoparticle. The magnetic hysteresis loops of the particle were measured at room temperature and a saturation magnetization of 56.8 emu/g was determined (a). Both r1 and r2 of the SPIO nanoparticle (0.1 mM in the water at 23 °C) were evaluated by a 0.3 T MR imager. The longitudinal relaxation time (T1) was reduced from 2117 ms for pure water to 408 ms (b), while the T2 relaxation time was reduced from 2039 to 108 ms (c). Inversion-recovery was prepared with a variety of inversion time from 10 to 5000 ms and the CPMG spin echo with a variety of echo time from TE = 10–400 ms.

Table 1 A comparison of T_1 and T_2 values of Gd-DTPA and the SPIO particle in water, which were measured using each pulse for refocusing in the multiecho sequence

Reagents	T_1	T_2
ddH ₂ O	2117 ms	2039 ms
Gd-DTPA	603 ms	559 ms
SPIO	408 ms	108 ms

shows the viabilities of both SMMC-7721 and HL7702 cells exposed to the ferrofluids at various iron concentrations. Cell viability was determined by using the 5-dimethylthiazol-2-yl-2, 5-diphenyl tetrazolium bromide (MTT) assay. The cells used for this purpose were fixed with 3% formaldehyde and washed with PBS, followed by the incubation with 2% potassium ferrocyanide in 6% hydrochloric acid for 30 min. After wash, the cells were counterstained with Giemsa solution. The viability of the cells was expressed as the mean \pm S.E. of the percentage of absorbance of controls where 100% equaled viability of untreated control cells. Prussian blue staining of the transfected cells showed the uptake of the SPIO nanoparticles in the cytoplasm (b) and no staining was observed in the cytoplasm of the cells transfected with Gd-DTPA (c) and the no-transfected SMMC-7721 (d). In addition, the SPIO nanoparticles were administrated into the Wistar rats via lateral tail vein at a dose 10mg/kg for hemolysis assay (Weissleder et al 1990). The number and morphology of blood cells were evaluated 24 h later (e and f) and the feedback of the rats in the following 3 months was examined. These data strongly suggested that the SPIO nanoparticle would be generally considered to be biocompatible.

Magnetic resonance imaging

Animals were purchased from Shanghai SLAC laboratory animal Co. LTD and a hepatoma model of rat was developed with DEN as described elsewhere (Mathew et al 1980; Williams et al 1996). MRI examinations were performed on a 1.5 T GE tweenspeed MR imager using a commercially available extremity 7.6 cm coil.

To evaluate the potential of the SPIO nanoparticle in clinical MR imaging further, the signal intensity alterations

Table 2 The relaxivities of Gd-DTPA and the SPIO nanoparticle at the same magnetic field strength

Samples	Magnetic field strength (T)	r1 (L/mmol.sec ⁻¹)	r2 (L/mmol.sec ⁻¹)	r2/r1
Gd-DTPA	0.3	11.86	12.98	1.09
SPIO	0.3	19.79	87.69	4.43

influenced by interactions between nanoparticles and water or whole blood were analyzed using different imaging sequences. Serial 10-fold dilutions of the SPIO nanoparticles were prepared in the deionized water and human whole blood to the final concentrations, ranging from 10^{-2} to 10^{-7} M. The same concentration gradients of Gd-DTPA were also prepared for comparative observation. 1.5 ml of each preparation was loaded into an array of 1.5 ml Eppendorf tubes in a plastic rack. The image was taken using the designed sequences by 3 acquisitions with the field of view being 80×80 mm². The parameters for T1 image was spin echo (SE) with repetition time (TR) 460 ms, echo time (TE) 9.0 ms in a matrix size of 512×512 , for T2 image was fast spin echo (FSE) with TR/TE = 3000 ms/70.1 ms, echo train length (ET) = 17 ms in a matrix size of 256×256 and for T2 weighted image was gradient echo with TR/TE/flip angle = 340 ms/17ms/ 30 in a matrix size of 512×512 . The signal intensity of each sample was determined by standard region-of-interest measurements of cross sectional image of each individual tube using the provided image quantification tool. In Figure 4, the representative images from T1 (a), T2 (b) and T2W (c) revealed that MR signal intensity was affected by the ion concentrations of the two contrast agents. The dispersion of the SPIO nanoparticle in an array of concentration gradient of human whole blood ranged from 10^{-2} to 10^{-5} M iron concentration showed significant decreasing of signal intensity at 10^{-3} M (d), especially in T2 weighted MR image. In vitro MR images of SPIO nanoparticles were highly consistent with the results of r1 and r2 measurements described above.

For the application of the SPIO nanoparticle to detect hepatoma nodules, the rats were anesthetized for MR imaging by means of intramuscular injection of 50 mg/kg ketamine hydrochloride and the contrast medium was injected into a lateral tail vein. As the USPIO nanoparticles have a prolonged blood half-life, the SPIO nanoparticles were used the last to avoid any residual effect on the studies when performed with the Gd-DTPA. The parameters for T1 image was spin echo (SE) with repetition time (TR) 460 ms, echo time (TE) 9.0 ms in a matrix size of 512×512 , for T1 weighted image was SE with TR/TE = 420 ms/9.0 ms in a matrix size of 256×256 , for T2 image was fast spin echo (FSE) with TR/TE = 3000 ms/69.9 ms, echo train length (ET) = 17 ms in a matrix size of 256×256 and for T2 weighted image was gradient echo with TR/TE/flip angle = 340 ms/17 ms/ 30 in a matrix size of 512×512 . In addition, a concentration of SPIO nanoparticles at 0.18 mmol Fe/kg was employed for in vivo studies, which roughly corresponds to a dose of 0.07

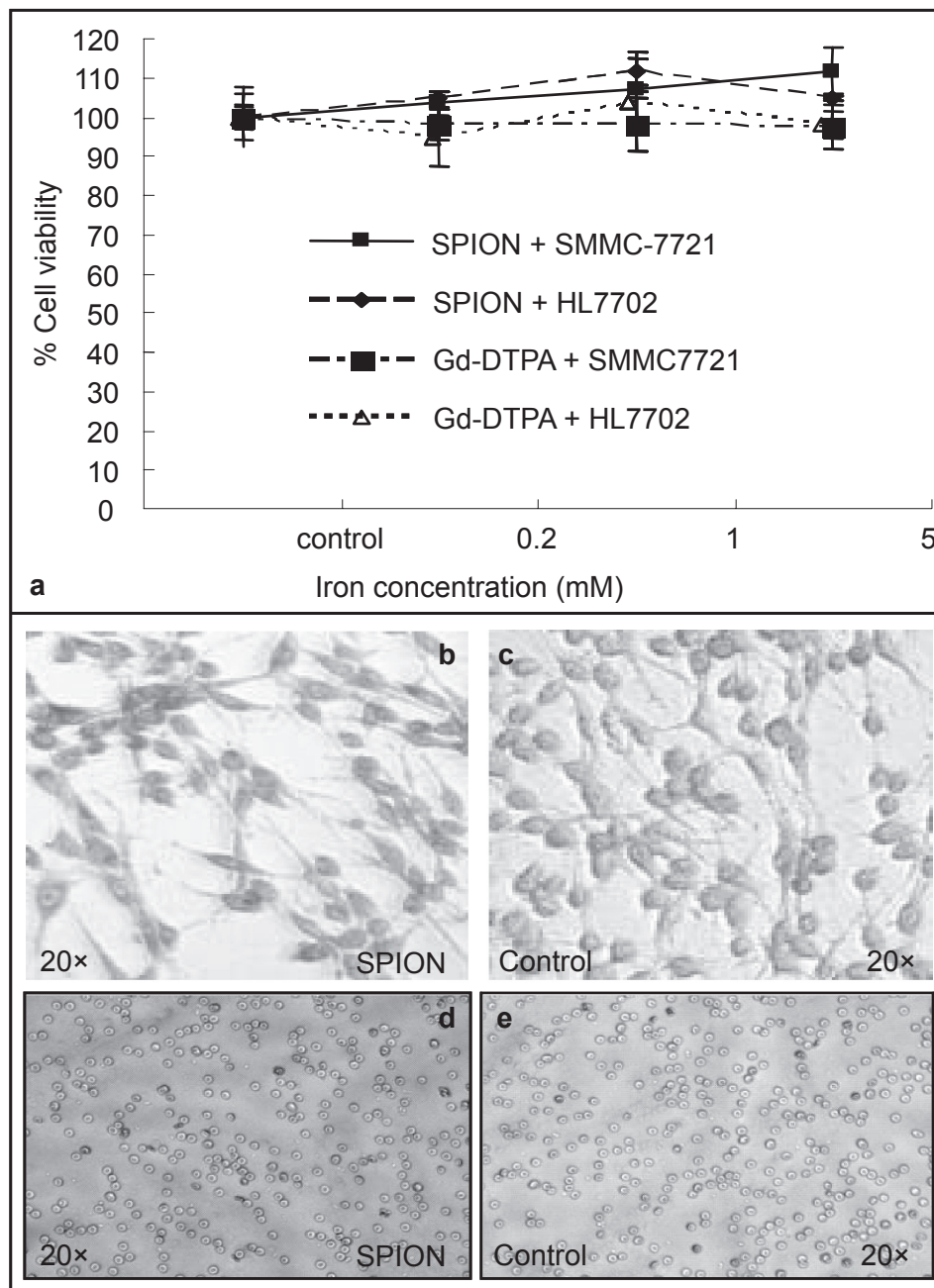


Figure 3 Evaluation of the cytotoxicity of the SPIO nanoparticle both in vitro and in vivo. Two human hepatic cell lines were employed for MTT assay (a). Prussian blue staining of the transfected cells showed the uptake of the SPIO nanoparticles in the cytoplasm (b), and no staining was observed in the cytoplasm of the cells transfected with Gd-DTPA (c) and the no-transfected SMMC-7721 (d). In addition, hemolysis assay was carried out and no adverse effects on red blood cells regarding its number and shape 24h later following systemic administration of the nanoparticles (10mg/kg) in rats (e, the dilution of isolated RBCs was 1:200). Our results demonstrated that the prepared SPIO nanoparticle would be biocompatible.

mmol Fe/kg assuming that the blood volume is 70 ml/kg b.w. in mammals. This dose results in increasing T2 shortening, which led to negative enhancement or “black-out” of the liver (Figure 5b). As a result, the SPIO nanoparticle was used for MRI detection of hepatoma nodules around 1mm in diameters in the liver of rats (Figure 5b). In Figure 6, HCC lesions in a rat liver showed low signal intensity on the T1-weighted SE (Figures 6a and 6c) and isointensive nodules on the T2-

weighted SE (Figures 6b and 6d). All the MRI findings were further confirmed by necropsy and histological examinations. The Gd-DTPA was used for comparative observation (Figures 6e and 6f).

Discussion

Betaine is a liver-born S-adenosylmethionine (SAM) generator with active surface property. It has been known

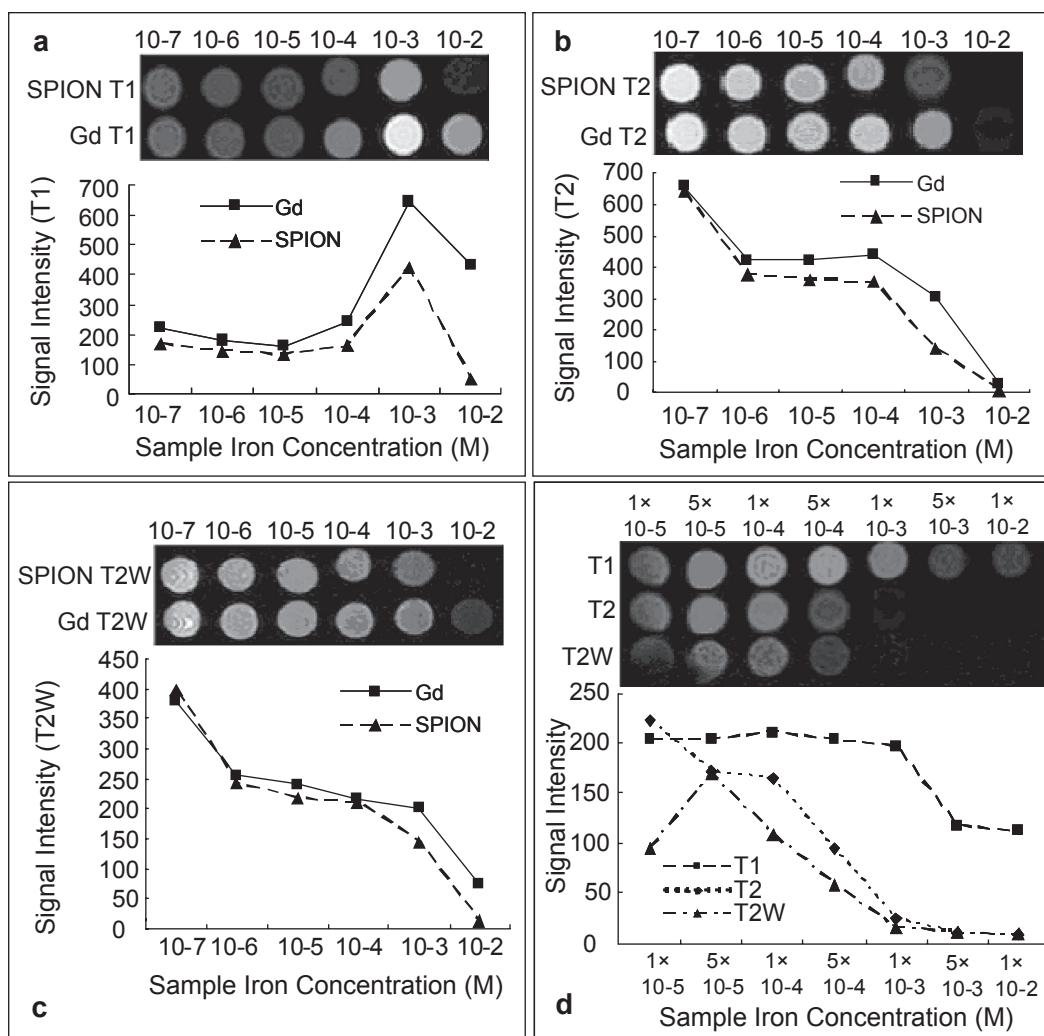


Figure 4 The signal intensity alterations influenced by interactions between nanoparticles and water or whole blood were analyzed using different imaging sequences. The samples were diluted in water or human whole blood at different concentrations. The representative images of Figures 1a and 1b were acquired from T1 and T2 respectively. The T2 weighted MR signal intensity was affected by the ion concentrations of the two contrast agents (c). The nanoparticle in human whole blood ranged from 10⁻² to 10⁻⁵ M. Significant decreasing of signal intensity at 10⁻³ M, especially in T2 weighted MR image, was observed (d).

that betaine is involved in the reaction of methionine metabolism in mammalian liver and it is a promising alternative to expensive SAM agent in the treatment of liver dysfunction and other human maladies (Barak et al 1996). Taking the advantage of betaine as a liver-born SAM generator with active surface property, we hypothesized that betaine modification could change both the physical and biological properties of the nanoparticles and thereby would offer improvement of their biosafety profiles and pharmacokinetic properties.

There are two recent reports of non-polymer coated SPIO nanoparticles. The VSOP-C91 (Ferropharm, Teltow, Germany) coated with a citrate monomer is characterized by a favorable ratio of T2 relaxivity (r2) to T1 relaxivity (r1) in combination with a long blood pool half-life (Reimer et al 1992; Chouly et al 1996). In another study, a SPIO nanopar-

ticle incorporated with (CH₃)₄N⁺ was investigated using a 1.5 T clinical MR imager, in which significant reduction of the background medium signal was found in the T2-weighted and the T2*-weighted sequence in the serum and whole blood (Taupitz et al 2002) *in vitro*. In our approach, the SPIO nanoparticles were stabilized by betaine monomer and were systematically investigated both *in vitro* and *in vivo*.

Kinetic studies of the liver MR contrast agents suggest that hydrophobic surface may enhance the uptake of the nanoparticles by the liver, while hydrophilic coating and surface charges may influence their retention period in the circulation (Taupitz et al 2000; Schnorr et al 2002; Wagner et al 2002). In this study, we found that the betaine coated SPIO nanoparticle presented significant reduction of the background signal in the T2-weighted sequence, which led to adequate performance in the detection of hepatoma nodules varied 1~25 mm at a low

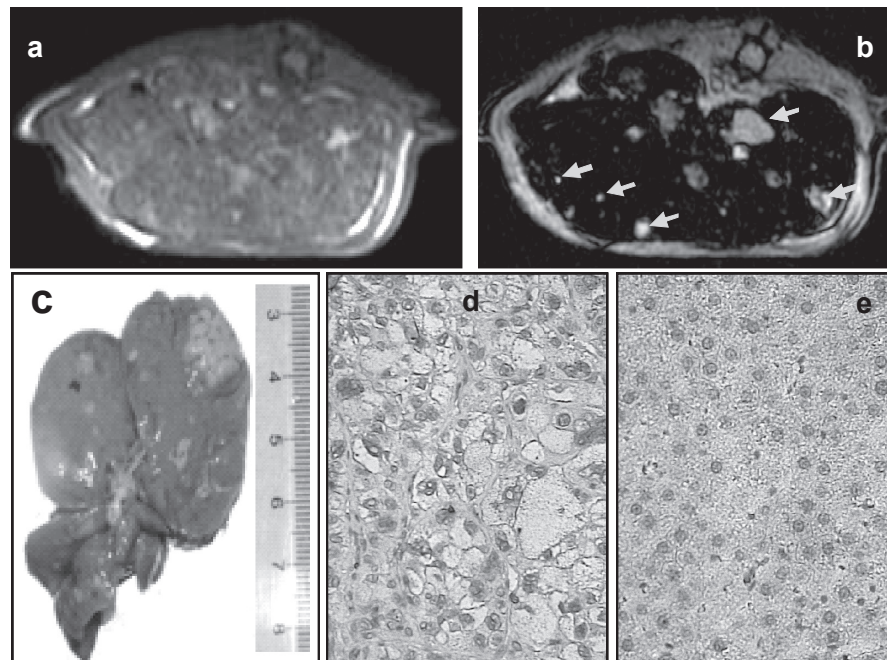


Figure 5 MR image and histological examination of hepatoma nodule in a rat model. Following administration of SPIO nanoparticles 45 min, MR images for the almost same axial slice of the liver on the T1-weighted SE (a) and on the T2-weighted SE (b) were performed. On the T2-weighted SE MR image, the enhancement of negative signals of liver and small nodules isointensive to liver was found. At necropsy 1h later after MRI, hepatoma nodules were found in the liver of rat (c). Hematoxylin staining of the resected paraffin specimen from the rat showed well-differentiated hepatoma cells (d), comparing with normal controls (e). The histological results confirmed the MRI and necropsy findings further.

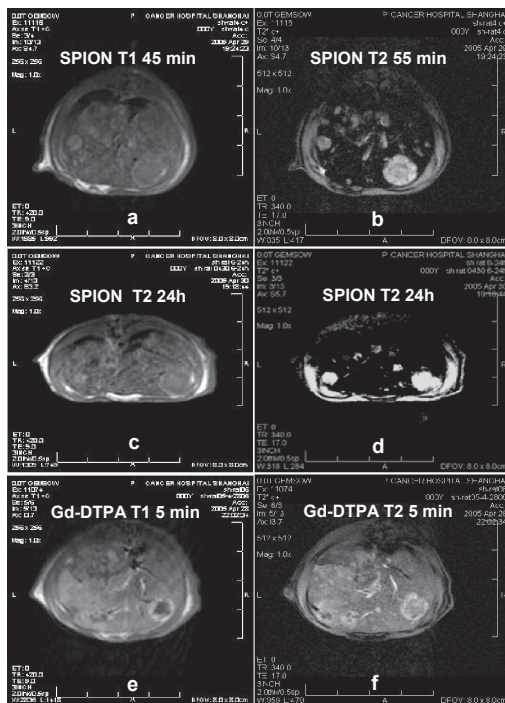


Figure 6 MR images of hepatoma lesions in a rat liver. Following administration of SPIO nanoparticles 45 min and 24 hours later, the hepatoma nodules were shown low signal intensity on the T1-weighted SE (a and c), isointensive nodules were found on the T2-weighted SE (b and d). The Gd-DTPA was used as a control (e and f). To avoid any residual effect on the study, the SPIO nanoparticles were administered 48 hours later following injection of the commercial Gd-DTPA.

dose. In addition, the nanoparticles fabricated in the water phase have additional advantages over those synthesized in the organic phase or those required additional polymer protection for stabilization. This could not only provide a more physiological reaction background for the tagged biomolecules, but have distinct biodistribution and metabolic clearance profile than the conventional polymer coated particles. Moreover, betaine modification could improve the biosafety profiles of the SPIO nanoparticle and could be a promising SAM carrier for the treatment of some liver dysfunction.

Acknowledgments

The authors would like to thank Dr. Jianqi Li in Department of Physics, East China Normal University, Dr. Weijun Peng in Department of Radiology, Cancer Hospital of Fudan University, for their assistant to performing MRI. This work was supported by Shanghai metropolitan fund for research and development (04DZ14005 and 04JC14096) and by key programs of NSFC (30430240).

Author's Contribution

Lin Du and Jianzhao Chen Contributed equally to this work.

References

- Barak AJ, Beckenhauer HC, Tuma DJ. 1996. Betaine, ethanol and the liver: a review. *Alcohol*, 13:395–8.
- Cheng F-u, Su C-H, Yanga Y-S, et al. 2005. Characterization of aqueous dispersions of Fe₃O₄ nanoparticles and their biomedical applications. *Biomaterials*, 26:729–38.
- Chouly C, Pouliquen D, Lucet I, et al. 1996. Development of superparamagnetic nanoparticles for MRI: effect of particle size, charge and surface nature on biodistribution. *J Microencapsul*, 13:245–55.
- Gupta AK, Gupta M. 2005. Synthesis and surface engineering of iron oxide nanoparticles for biomedical application. *Biomaterial*, 26:3995–4021.
- Hu XL, Yu JC. 2006. Microwave-assisted synthesis of a superparamagnetic surface-functionalized porous Fe₃O₄/C nanocomposite. *Chem Asian J*, 1:605–10.
- Mathew T, Karunanithy R, Yee MH, et al. 1980. Hepatotoxicity of dimethylformamide and dimethylsulfoxide at and above the levels used in some aflatoxin studies. *Lab Invest*, 42:257–62.
- Panyam J, Labhasetwar V. 2003. Biodegradable nanoparticles for drug and gene delivery to cells and tissue. *Adv Drug Del Rev*, 55:329–47.
- Reimer P, Kwong KK, Weisskoff R, et al. 1992. Dynamic signal intensity changes in liver with superparamagnetic MR contrast agents. *J Magn Reson Imaging*, 2:177–81.
- Schnorr J, Wagner S, Pilgrimm H, et al. 2002. Preclinical characterization of monomer-stabilized very small superparamagnetic iron oxide particles (VSOP) as a blood pool contrast medium for MR angiography. *Acad Radiol*, 9(Suppl 2):S307–9.
- Taupitz M, Schnorr J, Abramjuk A, et al. 2000. New generation of monomer-stabilized very small superparamagnetic iron oxide particles (vsop) as contrast medium for angiography: preclinical results in rats and rabbits. *Journal of Magnetic Resonance Imaging*, 12:905–11.
- Taupitz M, Schnorr J, Wagner S, et al. 2002. Coronary MR angiography: experimental results with a monomer-stabilized blood pool contrast medium. *Radiology*, 222:120–6.
- Thünemann AF, Schütt D, Kaufner L, et al. 2006. Maghemite nanoparticles protectively coated with poly (ethyleneimine) and poly (ethylene oxide)-block-poly(glutamic acid). *Langmuir*, 22:2351–7.
- Wagner S, Schnorr J, Pilgrimm H, et al. 2002. Monomer-coated very small superparamagnetic iron oxide particles as contrast medium for magnetic resonance imaging: preclinical in vivo characterization. *Invest Radiol*, 37:167–77.
- Weissleder R, Elizondo G, Wittenberg J, et al. 1990. Ultrasmall superparamagnetic iron oxide: characterization of a new class of contrast agents for MR imaging. *Radiology*, 175:489–93.
- Wilkinson JM. 2003. Nanotechnology applications in medicine. *Med Device Technol*, 14:29–31.
- Williams GM, Iatropoulos MJ, Wang CX, et al. 1996. Diethylnitrosamine exposure-responses for DNA damage, centrilobular cytotoxicity, cell proliferation and carcinogenesis in rat liver exhibit some non-linearities. *Carcinogenesis*, 10:2253–8.
- Zhang Y, Kohler N, Zhang M. 2002. Surface modification of superparamagnetic magnetite nanoparticles and their intracellular uptake. *Biomaterials*, 23:1553–61.